

Relating reflectance spectra space to Munsell color appearance space

A. Kimball Romney

Institute of Mathematical Behavioral Sciences, University of California, Irvine, California 92697-5100, USA
 akromney@uci.edu

Received June 18, 2007; revised October 31, 2007; accepted December 20, 2007;
 posted January 9, 2008 (Doc. ID 84246); published February 13, 2008

The goal is to construct a simple model relating the conceptually defined Munsell color space to a physical representation of the relationship among the reflectance spectra obtained from the color chips comprising the Munsell color atlas. In the model both the Munsell conceptual system and the transformed reflectance spectra are shown to be well represented in Euclidean space, and the two spaces are related by a simple linear transformation. A practical implication is that the method allows one to compare the location of an empirical reflectance spectrum with the aiming point in the conceptual structure. © 2008 Optical Society of America
 OCIS codes: 330.0330, 330.1690, 330.1710.

1. INTRODUCTION

Traditional color research is based on the assumption that the color appearance of color chips originates in their reflectance spectra that, together with the illumination source, determine the light stimuli reaching the photoreceptors of some specified standard observer [1]. In contrast, we focus attention on a highly constrained context, namely, the appearance of the color of a single color chip observed on a neutral background in normal daylight. This constrained context is free of complex context effects such as color contrast, color induction, and other complicating phenomena. The physical information about a color sample in such a constrained context resides in the measured reflectance spectrum. Reflectance spectra are typically obtained by illuminating the sample with a standard light as near equal as possible at all wavelengths and measuring the percent of light reflected from the sample at each wavelength. We assume that two samples with identical reflectance spectra will appear the same when judged by humans in the constrained context. This is in accord with Billmeyer and Saltzman [2], who say that two color samples comprise an invariant match when they have identical reflectance spectra and that such invariant matches look alike to all observers under all light sources. Since the data used in this paper are derived from color chips, in which the relative relationship among the chips is a function of their reflectance spectra, illumination and observer characteristics do not appear in the model. We should stress that the model developed below is a mathematical simplification that has no relationship to how biological organisms actually compute color appearance.

Our formulation of the relation between reflectance spectra (preceded by a cube root transformation for reasons to be discussed below) and color appearance systems begins with an empirical finding and an observation. First, we find that transformed reflectance spectra of the Munsell [3] color atlas chips are well represented in three-dimensional Euclidean space. We designate the em-

pirically derived coordinates of this space the reflectance spectra space. Second, we observe that the conceptual structure underlying the Munsell color chips may be perfectly represented in a three-dimensional Euclidean space. The Euclidean coordinates of the aiming points in this geometrically defined structure we designate as Munsell space. The aim of the paper is to provide a simple model that provides formulas for computing transformations between these two spaces that maintains the integrity of the internal shape of each of the spaces.

The organization of the paper is as follows: We begin with a sketch of how the Munsell space was developed and perfected by the Optical Society of America, including how the atlas was actually produced. The description of the Munsell color space concludes with a specification of the aiming points for the atlas color chips defined in Euclidean coordinates. We then briefly review some previous studies of the basis functions and representations of the global structure of the Munsell system. These preliminaries lead to the major findings of the paper, which consist in the derivation of the model of transformations between the reflectance spectra space and the aiming points of the conceptual Munsell space. Following the development of the model, we discuss some further implications of the model and conclude with a short summary.

2. BRIEF REVIEW OF MUNSELL CONCEPTUAL COLOR SYSTEMS

During the middle decades of the past century, the Optical Society of America sponsored an ambitious attempt to design a color appearance system that led to the *Munsell Book of Color* [3]. Excellent descriptions of the Munsell system may be found in Wyszecki and Stiles [1] and Newhall *et al.* [4]. The system was based on extensive research involving over three million psychophysical judgments with the aim of producing an atlas of sample color chips covering as wide a gamut as possible over the real-

izable color space in regular perceptual steps according to a specified geometry. One result of these efforts led to the 1976 version of the Munsell atlas, consisting of 1269 2 in. (1 in=2.54 cm) square painted chips

The organization of the conceptual Munsell system is organized around the concepts of value, hue, and chroma. Before describing the detailed geometry of the Munsell space, it will be useful to review the development and production of the actual painted chips. Our description is based on the detailed report by Davidson and Hemmendinger [5] of how an early version was produced. The aiming point for the color location of each chip was first conceptualized in terms of the Munsell conceptual system. The definition of the aiming points were estimates; there were no absolutely secure anchor points. All paints used in the production of the chips were mixed from just six colored paints (yellow, orange, red, red-purple, blue, and green) plus black and white. Only two colors of paint were combined to produce any given hue, and variations in value and chroma were produced by the addition of black and white paint as needed. Over a thousand combinations were painted as a first step in the calibration process. The resulting samples were measured and located in CIE space. With this information the painter drew charts by hand to help estimate the mixture of paints required to obtain a color chip that corresponded to a specified location in the CIE estimate of the conceptual Munsell space. The result was a set of painted color chips that conforms reasonably close to the Munsell conceptual system. Independent studies confirm the approximately equal perceptual spacing of the color chips and the overall organization of the system [6,7].

In the Munsell conceptual system, value is generally taken to be the vertical dimension and varies from 2.5 (dark) to 9 (light). At each value level, 40 spokes representing hues radiate out from a central achromatic axis in circles of increasing chroma beginning at one and continuing with even integers. The full set of color chips in the Munsell system may be represented as a somewhat irregular sphere, as shown in Figs. 1(a)–1(c). The colors in the plot reflect the major hue sectors named below and are otherwise arbitrary. The actual colors range from near black to near white on the vertical value (lightness) axis and from achromatic to higher chroma (saturation) as color chips depart farther from the achromatic locus of the

circles. Viewed from above, as in Fig. 1(c), the various hues are seen as 40 spokes radiating out from the achromatic central axis. The circles of increasing size represent increasing levels of chroma. The size of each chroma circle is invariant through all levels of value, and they are stacked on top of each other to form cylinders. There are ten equally spaced hue sectors labeled red, red-purple, purple, purple-blue, blue, blue-green, green, green-yellow, yellow, and yellow-red. The four spokes in each sector represent finer hue gradations, called areas in the Munsell system, labeled 2.5, 5, 7.5, and 10. Area 5 usually represents the most representative hue. Fig. 1(a) shows a full plot of the two pages of the Munsell color system that constitute the spokes of the 5 green-blue versus 5 red axis, while Fig. 1(b) shows those of the 10 blue-purple versus 10 yellow axis. From psychophysical evidence Indow [6,7] has shown that one value step in this system is roughly equivalent to two chroma steps. To adjust for this we have arbitrarily divided the chroma scale by two and fit the aiming points of the conceptual Munsell system into the Euclidean coordinates accordingly; thus in the plots using Munsell coordinates, the chroma numbers shown need to be doubled to get the correct Munsell chroma levels. Procedures for obtaining the Cartesian coordinates are described in D'Andrade and Romney [8] and have been used in previous papers [9–12].

3. PREVIOUS STUDIES OF REFLECTANCE SPECTRA AND GLOBAL STRUCTURES

In this section we look at examples of previous studies of two kinds: The first focused on reflectance spectra and the question of how many basis functions are needed for an adequate representation, and the second focused on the analysis of the relation among reflectance spectra as represented in some global geometrical structure. Some studies have included results on both basis functions and global structure.

The first study of the basis functions of reflectance spectra is that of Cohen [13]. He published the mean and first four basis functions in 1964 based on a sample of 150 Munsell chips measured in 10 nm intervals over the range of 380 nm to 770 nm. The first three accounted for over 0.99 of the overall variance. Maloney [14] used these basis functions to estimate multiple correlation coeffi-

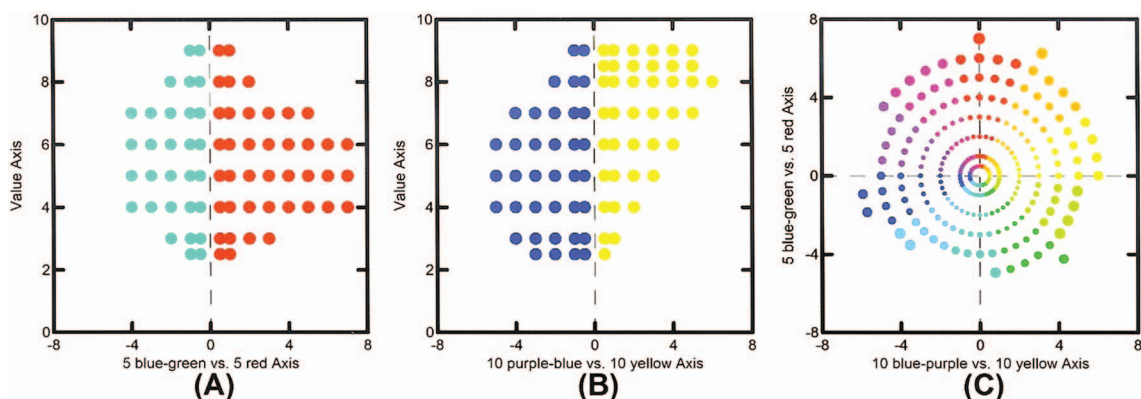


Fig. 1. Conceptual Munsell color system represented in Cartesian coordinates with arbitrary color coding meant to convey hue locations in an approximate fashion.

cients of the spectra of an expanded set of 462 Munsell chips as well as 337 natural objects. He found median values of over 0.996 for the Munsell reflectance spectra using three basis functions, confirming the results of the overall fit. Maloney clearly established that reflectance spectra were broadband and generally smooth over the range of 400 to 700 nm. He speculated that there were physical constraints imposed on the band limits of reflectance spectra by molecular interactions and the superimposed vibrational/rotational patterns [14]. More recently, Maloney [15] has studied the spectra in more detail and estimates that more than three dimensions are necessary, even though well over 0.98 of the variance is accounted for in three dimensions. In addition to an extended set of Munsell color chips, Romney and Indow [9] analyzed the same reflectance spectra of natural objects included in Maloney's [15] study and concluded that only three, or at most four, dimensions were required for an adequate fit. Jaaskelainen *et al.* [16] show a plot of the first three basis functions of 1257 Munsell color chips that is very similar to what others have found, although they think that it may be necessary to use more than three to obtain precise accuracy. Dannemiller [17] has analyzed the number of basis functions necessary to represent the reflectance spectra of natural surfaces as represented in the Krinov [18] data and concludes that three basis functions are necessary and probably sufficient for representing the spectral reflectance functions of natural objects [17].

Lenz *et al.* [19] made a detailed study of three collections of reflectance spectra, two Munsell and one on the Natural Color System, and found that the first few eigenvectors are almost identical for all three databases. Chiao *et al.* [20] conducted a study of reflectance spectra collected from images of natural scenes of both forests and coral reefs. Their plots of the basis functions have a qualitative similarity to those obtained from color chips, and the first three account for about 98% of the total variance. In all these various studies on the basis functions of the reflectance spectra of color chips and various natural objects, it is clear that the shapes of the first three or four basis functions are qualitatively similar from study, to study although there is no complete consensus on the exact number of basis functions necessary in practical applications.

The second category of studies has focused on how to relate reflectance spectra to the global appearance of color space. Some utilize just the reflectance spectra, while others include some data on an assumed observer. We discuss those based on just reflectance spectra first. Koenderink and van Doorn [21] present an idealized spherical configuration of color space obtained by singular value decomposition but do not show the empirical evidence for the structure. Lenz and Meer [22] analyzed a database consisting of reflectance spectra of 2782 color chips. They find that the data described by coordinate vectors lie in a cone, and they therefore define a hyperbolic coordinate system to represent the data and present a three-dimensional figure of the distribution of the chips. Usui *et al.* [23] construct a three-dimensional representation of Munsell color space using a five-layer neural network that is qualitatively similar to one obtained with singular value decomposition.

Another category of global representations of reflectance spectra uses observer-based models that utilize some observer characteristic, such as a standard observer based on color matching functions or cone receptor curves, making an observation of a color chip under some specified source of illumination. For example, color matching functions were used in the first analysis of the global structure of the Munsell reflectance spectra done by Burns *et al.* [24]. They mapped Munsell reflectance spectra into what they call fundamental color space, which is basically a projection of the reflectance spectra through the color matching functions. They used the interval from 380 nm to 770 nm and obtained very clear representations of the Munsell conceptual structure. Since they did not use any nonlinear transformations, their Munsell value intervals were unevenly spaced and their chroma circles expanded as lightness levels increased. Laamanen *et al.* [25] used the cone response curves of Smith and Pokorny to model the Munsell color chips. They obtain very satisfactory fits to the Munsell conceptual system using an optimization program. They also provide a most useful and up-to-date review of significant studies relating reflectance spectra of Munsell color chips to the global color space that need not be duplicated here.

In our own work with Indow [9] we originally reported a Euclidean representation of the reflectance spectra of Munsell color chips obtained with classical multidimensional scaling methods. Subsequently, we showed [11] that the row vectors weighted by the singular values obtained from a singular value decomposition of reflectance spectra result in a Euclidean representation of Munsell color chips. The fit was poor since value levels were spaced unevenly and chroma increased with value. Working with D'Andrade [8], we attempted to transform the physical description of the Munsell chips into the Munsell color system using D65 illuminant and the Stockman and Sharpe cone sensitivity curves. That model, which accounted for about 98% of the data, used a cube root transformation that produced evenly spaced value levels with equal intervals of chroma at all levels. In a recent paper with Fulton [12] we found that four independent methods of fitting the reflectance spectra of Munsell chips to the Munsell conceptual system converged to a common solution to within a fraction of a percent. The four methods were based on the following approaches: (a) the CIE L*a*b* international standard, (b) the D'Andrade and Romney model [8] using Stockman and Sharpe cone sensitivity curves, (c) the cube root of the sums of the products of reflectance spectra and synthesized prime color curves, and (d) a simple transformation of a Euclidean representation obtained with singular value decomposition of cube rooted spectra. The four methods gave results much closer to one another than any was to the theoretical locations defined by the Munsell system, suggesting that taking into account the illuminant and standard observer or cone sensitivity curves, as in approaches (a) and (b) above, does not add any precision in estimating color appearance in a restricted context such as color samples from a color atlas. In this paper we develop a model suggested by but distinct from approach (d) above. In a previous paper [12] we simply regressed the coordinates derived from the cube rooted reflectance spectra to fit the

Munsell coordinates. In the model below we first synthesize idealized reflectance spectra from the Munsell coordinates and then work back from these to obtain exact estimates of the Munsell aiming points. The details of how this is done will be shown below.

4. TRANSFORMATIONS BETWEEN REFLECTANCE SPECTRA SPACE AND CONCEPTUAL SPACES

The reflectance spectra analyzed in this paper derive from 1269 spectra of the 1976 matte edition of the Munsell color atlas [3]. The spectra were obtained from a Perkin–Elmer lambda 9 UV/VIS/NIR spectrophotometer measured from 380 nm to 800 nm at 1 nm resolution using an integrative sphere. The source of the data and information on the usefulness of this and other data sets are described in Kohonen *et al.* [26]. Since color vision research is usually based on a range of 400 nm to 700 nm, we use the reduced range and represent these data as a matrix, $\mathbf{A}_{1269 \times 301}$.

It has been long established that a nonlinear transformation is necessary to transform reflectance spectra into a reasonable approximation of a perceptual color system. The international color standard CIE $L^*a^*b^*$ [1] uses the cube root transformation, and our findings in previous research [8,12] provide additional evidence that the cube root is the appropriate transformation for modeling perceptual color space. It may also be noted that the fifth-

order polynomial defining the Munsell renotation value scale is plotted as indistinguishable from the CIE 1976 lightness function that uses the cube root transformation [see Fig. 2(6.3) in [1]]. In this paper we apply the cube root transformation to the reflectance spectra prior to further analysis. The effect of this transformation is illustrated in Fig. 2, where untransformed spectra are shown in the left column, spectra transformed by taking the cube root are shown in the middle column, and ideal spectra derived from Munsell coordinates, obtained with procedures described below, are shown in the right column. The four rows of Fig. 2 represent samples from the four Munsell hues that form the axes of Fig. 1. The spectra contain all values of lightness of chips of chroma 6. Thus the spectra in a single panel differ only in lightness. Note that the untransformed spectra in the first column have noticeable differences in the shape and spacing of the curves. For the cube root spectra in the middle column, the curves are of the same general shape and nearly equally spaced. The observed discrepancies from perfect equality in spacing and shape may arise from various sources such as design errors in translation from CIE specifications to Munsell aiming points, errors in hand-drawn templates by Davidson and Hemmendinger [5], errors in weighing the combinations of paints, etc. The reflectance spectra in Fig. 2 are representative of painted surfaces in general in that they are very broadband and relatively smooth curves that reflect at least some light at all wavelengths. Although this is true of painted surfaces such as the Mun-

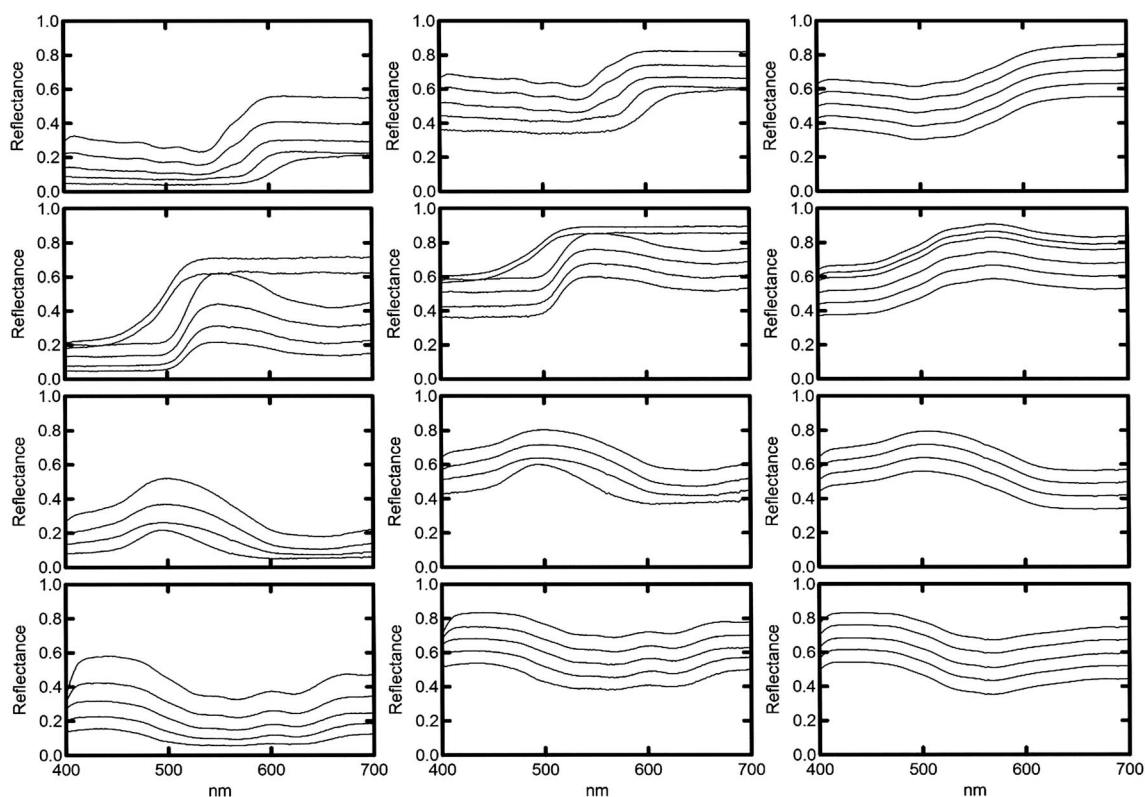


Fig. 2. Sample illustrations of reflectance spectra of all varying values that occur at chroma level 6 of four equally spaced Munsell hues, where untransformed spectra are shown in the left column, spectra after cube root transformations are shown in the middle column, and reconstructed transformed reflectance spectra of the ideal conceptual Munsell chips are shown in the right column. The Munsell hues represented in the four rows are, starting at the top, 5 red, 10 yellow, 5 blue-green, and 10 purple-blue.

sell chips, many natural objects [27], and a variety of chemicals and pigments [28–30], its full generality remains to be determined.

Note in the right-hand column of Fig. 2, in which the idealized Munsell spectra are modeled, that two pairs, namely, 5 red versus 5 blue-green and 10 yellow versus 10 purple-blue, have complementary shapes and at appropriate value levels correspond perfectly when superimposed with one of the pairs reflected in the vertical dimension. This corresponds to the structure of the Munsell color system, in which complementary colors combine to form achromatic shades of gray centering on the zero point of the axes.

We turn now to the task of representing the reflectance spectra in Euclidean space. Based on the discussion above, we take a cube root, elementwise, of the original matrix, to obtain

$$\mathbf{S}_{1269 \times 301} = \sqrt[3]{\mathbf{A}}_{1269 \times 301}. \quad (1)$$

The main results reported in this paper derive from the analysis of the matrix $\mathbf{S}_{1269 \times 301}$.

Romney and Indow [9] demonstrated that a singular value decomposition of a matrix such as $\mathbf{S}_{1269 \times 301}$ provides a representation of the spectra as combinations of basis functions and a Euclidean representation of the physical relation among Munsell chips consisting of the singular row vectors multiplied by the singular values. In general, singular value decomposition analyzes a matrix such as $\mathbf{S}_{1269 \times 301}$ in the following way:

$$\begin{aligned} \mathbf{S}_{N \times M} &= \mathbf{U} \mathbf{\Delta} \mathbf{V}^T, & N \geq M \geq K, & \quad \mathbf{U}_{N \times K} = (u_{ik}), \\ & & & \quad \mathbf{V}_{M \times K} = (v_{jk}), \quad k = 1, 2, \dots, K, \end{aligned} \quad (2)$$

where $\mathbf{\Delta}$ is a diagonal matrix consisting of singular values d_k .

In our case, we find that $K=3$ provides an adequate approximation between the two sides of Eq. (2), resulting in a three-dimensional Euclidean representation. We can write

$$\hat{\mathbf{S}}_{1269 \times 301} = \mathbf{U}_{1269 \times 3} \mathbf{\Delta}_{3 \times 3} \mathbf{V}_{3 \times 301}^T. \quad (3)$$

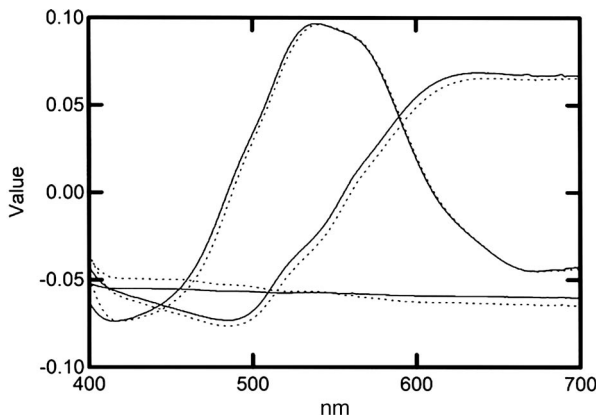


Fig. 3. Three basis functions computed from the Munsell reflectance spectra after cube root transformation, shown with solid curves, compared to the basis function derived from the original reflectance spectra, shown with dotted curves.

The adequacy of the approximation may be seen by comparing the sum of squares of the original data with that of the reconstructed data based on the first three basis functions. The sum of the squares of the full rank matrix, $\sum_{i=1}^{1269} \sum_{j=1}^{301} s_{ij}^2 = 152,520$, while the sum of squares of the three-dimensional reconstructed matrix, $\sum_{i=1}^{1269} \sum_{j=1}^{301} \hat{s}_{ij}^2 = 152,398$, indicating that the proportion of the sum of squares accounted for in the three-dimensional approximation is 0.9992. The same answer may be obtained as a proportion reduction in error measure or as the proportion of the sums of squares of the first three singular values compared to the sums of squares of the all singular values [31], namely,

$$\begin{aligned} \text{PRE} &= 1 - \frac{\sum_{i=1}^{1269} \sum_{j=1}^{301} (s_{ij} - \hat{s}_{ij})^2}{\sum_{i=1}^{1269} \sum_{j=1}^{301} s_{ij}^2} = \frac{\sum_{k=1}^3 d_k^2}{\sum_{k=1}^{301} d_k^2} \\ &= 0.9992. \end{aligned} \quad (4)$$

This result indicates that the cube roots of the Munsell reflectance spectra are well fitted in a three-dimensional Euclidean space and may be characterized by three basis functions, $\mathbf{V}_{3 \times 301}^T = \mathbf{V}_{301 \times 3} = \{\mathbf{v}_1, \mathbf{v}_2, \mathbf{v}_3\}$, from Eq. (3) and illustrated in Fig. 3 as solid curves. The dotted curves in Fig. 3 are the basis functions obtained from the original non-cube-rooted reflectance spectra and show that the transformation has little effect on the shape of the basis functions. All calculations were done with the program *Mathematica* [32]. The signs of the basis functions are arbitrary, and we report them as they emerged from the computer. The first basis function is close to a flat line or constant and represents the mean of the spectra and is roughly related to the Munsell value. In cases where the spectra are multiplied by an illuminant before processing, the first basis function is shaped like the illuminant [9]. All of the chromaticity information is contained in the second and third basis functions and accounts for differences in Munsell hue and chroma.

We next examine in detail the location of the chips in reflectance spectra space. The locations of the 1269 Munsell color chips represented in Euclidean reflectance spectra space may be estimated by weighting the row singular vectors by the singular values from Eq. (3) as follows:

$$\mathbf{P}_{1269 \times 3} = \{\mathbf{p}_1, \mathbf{p}_2, \mathbf{p}_3\} = \mathbf{U}_{1269 \times 3} \mathbf{\Delta}_{3 \times 3}. \quad (5)$$

These three vectors represent the contribution of each basis function to the estimation of any given spectrum. The \mathbf{p}_i for any given spectrum may be estimated with multiple regression techniques [33] similar in form to Eqs. (6)–(8) and (10)–(12) below; such coefficients are equivalent to those obtained by Eq. (5). Results showing the locations of the Munsell reflectance spectra are plotted in Figs. 4(a)–4(c). The various value planes visible in Figs. 4(a) and 4(b) are sloped rather than horizontal as in the conceptual Munsell. Figure 4(c) shows a plot of the second and third basis functions that have an overall qualitative similarity to the Munsell color system, even though it is not exactly centered on the zero point of the axes nor is it oriented the same, the whole figure being rotated about 20° to 30° counterclockwise.

The final task is to compute the relationship between the structure derived from an analysis of the reflectance

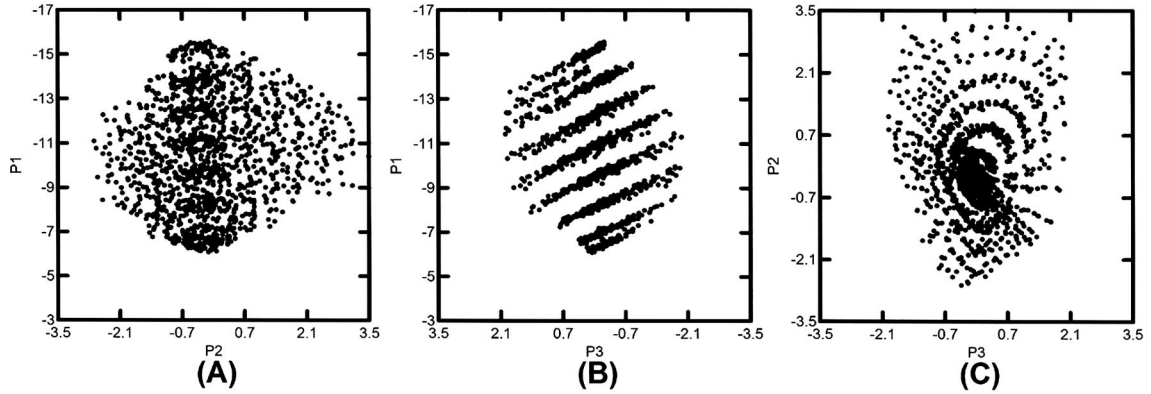


Fig. 4. Location of the Munsell color chips represented in Euclidean space as calculated using Eq. (5).

spectra and the conceptual Munsell structure. Our approach is to compute the linear transformation of the Munsell conceptual coordinates that best predicts the coordinates of the reflectance spectra space, namely, $\mathbf{P}_{1269 \times 3}$ from Eq. (5). We denote the Munsell conceptual coordinates as a matrix, $\mathbf{M}_{1269 \times 3} = \{\mathbf{m}_1, \mathbf{m}_2, \mathbf{m}_3\}$, where \mathbf{m}_1 = Munsell value, \mathbf{m}_2 = 5 red versus 5 green-blue Munsell axis, and \mathbf{m}_3 = 10 blue-purple versus 10 yellow Munsell axis. We obtain estimates of the Euclidean coordinates by standard regression techniques [33] and get estimates as follows:

$$\hat{\mathbf{p}}_1^m = -2.8204 + (-1.3423 \times \mathbf{m}_1) + (-0.1484 \times \mathbf{m}_2) + (0.2831 \times \mathbf{m}_3), \quad (6)$$

$$\hat{\mathbf{p}}_2^m = -0.0065 + (-0.0256 \times \mathbf{m}_1) + (0.4789 \times \mathbf{m}_2) + (0.2688 \times \mathbf{m}_3), \quad (7)$$

$$\hat{\mathbf{p}}_3^m = -0.2028 + (0.0395 \times \mathbf{m}_1) + (-0.1723 \times \mathbf{m}_2) + (0.2809 \times \mathbf{m}_3). \quad (8)$$

We substitute the estimated values of $\hat{\mathbf{p}}_i^m$ for those of \mathbf{p}_i in Eq. (5) and then use Eq. (3) to obtain estimates of the reflectance spectra of ideal conceptual Munsell samples. These estimates are obtained by the following equation:

$$\hat{\mathbf{S}}_{1269 \times 301}^M = \hat{\mathbf{P}}_{1269 \times 3}^M \mathbf{V}_{3 \times 301}^T. \quad (9)$$

In Fig. 2 we plot the reconstructed reflectance spectra $\hat{\mathbf{S}}_{1269 \times 301}^M$ in the right column for comparison to the empirically measured spectra. It may be seen that the spectra corresponding to the ideal conceptual Munsell chips in each panel are of the same shape and are equally spaced between the various value levels (except for the yellow panel, which contains an intermediate value level of 8.5.).

We now pose the question of where the empirical coordinates, $\mathbf{P}_{1269 \times 3}$, would be located in Munsell space. Since we know that the estimated $\hat{\mathbf{P}}_{1269 \times 3}^M$ matrix is a linear transformation of the Munsell coordinates, we can compute a linear transformation back to the Munsell coordinates as follows:

$$\mathbf{m}_1 = -1.9401 + (-0.7304 \times \hat{\mathbf{p}}_1^m) + (0.0235 \times \hat{\mathbf{p}}_2^m) + (0.7031 \times \hat{\mathbf{p}}_3^m), \quad (10)$$

$$\mathbf{m}_2 = -0.4825 + (-0.0719 \times \hat{\mathbf{p}}_1^m) + (1.5681 \times \hat{\mathbf{p}}_2^m) + (-1.4040 \times \hat{\mathbf{p}}_3^m), \quad (11)$$

$$\mathbf{m}_3 = 0.6990 + (0.0583 \times \hat{\mathbf{p}}_1^m) + (0.9286 \times \hat{\mathbf{p}}_2^m) + (2.5996 \times \hat{\mathbf{p}}_3^m). \quad (12)$$

Equations (10)–(12) apply not only to the hypothetical spectra generated by the ideal conceptual Munsell locations but to all possible spectra generated from the three basis functions. For example, to compute the location of

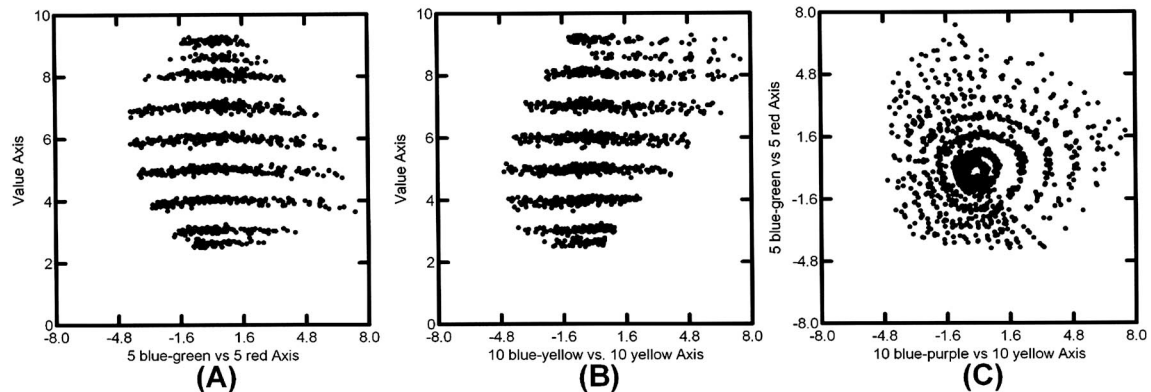


Fig. 5. Plot showing the location of the Munsell color chips after a linear transformation from the Euclidean system to the Munsell coordinate system. Orientation is the same as in Fig. 1.

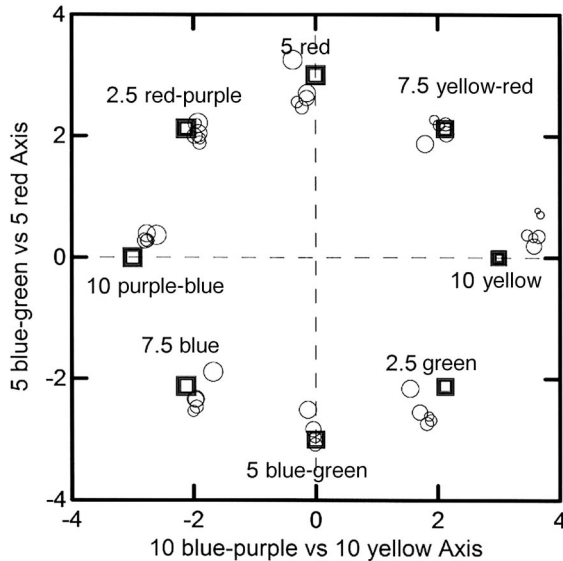


Fig. 6. Plot showing a comparison of the locations of selected empirical Munsell chips with their conceptual locations (after being transformed to Munsell space). The chips are eight equally spaced hues beginning at 5 red, all of chroma 6 with all degrees of value or lightness. The empirical locations are plotted as circles, while the conceptual locations are plotted as squares; the size of the symbols indicates value, with the largest circles being darkest. The thickness of the squares is produced by the superposition of symbols representing various values.

the empirically measured chips in Munsell space, we can substitute \mathbf{p}_i for the $\hat{\mathbf{p}}_i^m$ in Eqs. (10)–(12). Figure 5 shows the results of the linear transformation of the Euclidean model into the Munsell coordinate system. The similarity between Figs. 5 and 1 is striking and quantitatively close with only minor discrepancies.

The differences between the locations of the empirical chips in Fig. 5 from those of the ideal Munsell locations in Fig. 1 may have arisen from a variety of sources as noted earlier. To give an idea of the size and nature of the errors made, we plot in Fig. 6 the location of the spectra shown in Fig. 2 together with four additional intermediate hues. The locations of the empirical spectra from the middle column of Fig. 2 are plotted as circles, and the reconstructed conceptual spectra from the right column of Fig. 2 are plotted as squares. Note that chips of a given hue tend to be clustered and (except for yellow) outliers tend to be low in value (darkest colors are indicated by the largest circles), as may be seen by the fact that they are farthest from the center of the cluster. One of the advantages of the method presented here is that the direction and size of any error is immediately apparent. There is a cautionary message in Fig. 6 for experimenters using Munsell chips in color perception experiments. The assumption that the Munsell chips are located in their ideal conceptual locations would lead to errors of a magnitude equivalent to the errors illustrated in Fig. 6. These errors are large compared to the ability of humans to detect color differences.

5. FURTHER IMPLICATIONS OF THE MODEL

Alsam and Hardeberg [34] and Alsam and Finlayson [35] have recently applied the notion of convex sets to the so-

lution of two color problems: reducing the number of calibration charts and finding metamer sets without spectral calibration. The basic idea arises from the observation that reflectance spectra space and RGB space are closed and convex, and hence the extreme points in the data specify a convex hull that encloses the whole target. We propose to apply similar notions to enhance the usefulness of the model presented above. We proceed by generating all possible combinations of the three basis functions illustrated in Fig. 3 to construct a convex set of all reflectance spectra in the range from 400 nm to 700 nm that occur in the interval 0 to 1 to constitute a vector space defined as \mathbf{X} and $\mathbf{x}_i \in \mathbf{X}$. Within this set any combination [36] of elements from \mathbf{X} follows the rules of convex combination and is defined as a linear combination of the form

$$\alpha_1 \mathbf{x}_1 + \alpha_2 \mathbf{x}_2 + \cdots + \alpha_n \mathbf{x}_n, \quad (13)$$

where each $\mathbf{x}_i \in \mathbf{X}$, each $\alpha_i \geq 0$, and the α_i sum to 1.

Any proper subset of vectors that form a convex hull in the vector space of \mathbf{X} also follows the rule of convex combinations. The Munsell sample, $\mathbf{S}_{1269 \times 301}$, and its complement, $1 - \mathbf{S}_{1269 \times 301}$, computed elementwise, are proper subsets of \mathbf{X} . It follows that the rule of convex combinations is also valid in the space of $\mathbf{P}_{1269 \times 3}$ that specifies the weighting of the basis functions that form any specific reflectance spectrum. This space is embedded in a three-dimensional Euclidean space. An important implication of the linkage between the physical Euclidean space of reflectance spectra and the conceptual space of Munsell color by linear transformations is that solutions computed by convex combinations in either space apply equally well in both spaces. It is of interest to note that the paints used by Davidson and Hammendinger [5] to paint the Munsell chips constitute eight extreme points defining the convex hull of a convex set. Consequently, assuming the kind of stock used to produce the chips, the same paints, etc., the methods outlined in this paper could have been used to directly compute the appropriate combinations of paints to produce chips located in Munsell conceptual space.

The Munsell conceptual space has some practical advantages in the way the hues are arranged. One example, previously mentioned, is that the combination of any color (or its reflectance spectra) and its complement form an achromatic color (or constant spectra). Complementary colors in Munsell space also predict afterimage effects. The model also implies that if one were to use Munsell chips to replicate Maxwell's [37] experiments on the mixing of color samples with spinning discs, the results would be predicted by the rule of convex combinations calculated from the empirically obtained locations of the chips' reflectance spectra.

The question of the generality of the results needs to be addressed. In order to make a partial test of this question, we obtained the reflectance spectra of the Optical Society of America Uniform Color Scales (UCS) color chips. The geometric structure, which differs radically from the Munsell structure, is organized as a regular rhombohedral lattice embedded perfectly in three-dimensional Euclidean space and is well described by Wyszecki and Stiles [1]. We analyzed (calculations not shown) the 558 reflectance spectra using exactly the procedures applied to the

Munsell spectra and replicated the results almost exactly. The proportion of the sum of squares accounted for in the three-dimensional singular value decomposition was 0.9992 for the UCS, the same as for the Munsell data. These figures are based on the computation of independent basis functions for each data set. If one used a common set of basis functions to fit both sets, the overall figure would drop to 0.9991. The size of the discrepancies between the conceptual UCS locations and the empirically obtained locations from the reflectance spectra showed no detectable difference in magnitude from those reported above for Munsell. Davidson [38] presents a very detailed explanation of how the chips were painted, including specification of the 15 pigments and the actual reflectance spectrum of each. He also lists the actual composition of pigments of all 558 color chips and gives the source of the reflectance data. He indicates that even though there may be some inaccuracies, the chips should be good approximations of the specified UCS colors. It seems likely that the model presented in this paper may be generalized to color appearance atlases that are comparable to the Munsell and UCS in the sense that the conceptual aiming points are defined in a three-dimensional Euclidean space.

Finally, the construction of any color appearance atlas involves a kind of circularity that deserves comment. The Munsell conceptual system originated in the mind of Albert Munsell, who patented the system in 1906 (U.S. patent 824,374). The first atlas was, by necessity, an artist's invention of what color chip belongs in what location. The artist was informed, of course, by hundreds of years of accumulated folk knowledge. The problem of iterating back and forth between a conceptual system and actual colored chips was not easy, as illustrated by the decades of work the Optical Society of America invested in the Munsell renotation, the re-renotation, and the OSA UCS systems [1]. The circularity of previous systems has been imperfect in that small discrepancies have existed between the atlases and the conceptual systems on which they are based. In some sense this paper has demonstrated that a perfect circularity is possible in theory and has provided a method that should be of aid in approaching closer to that goal.

6. SUMMARY

The key conclusions of the paper are these: First, the cube rooted reflectance spectra of the Munsell color chips are well characterized in three-dimensional Euclidean space. Second, appropriate linear transformations provide a mapping between the Euclidean space of reflectance spectra and the Munsell conceptual space. Third, under proper constraints the three basis functions combine to describe a convex super set of realizable reflectance spectra that characterize colored surfaces, including painted and some other surfaces. Fourth, the rules of convex combinations apply to both the physical and conceptual spaces, and the linear transformations allow results obtained in one space to be applied in the other.

It is understood that the conditions in which these conclusions are valid are constrained to viewing color samples in a neutral achromatic background. If more

than one sample is viewed, it is further assumed that the samples are illuminated with the same source. In this restricted situation we assume that the measured reflectance spectra of the sample contain the relevant information for color description. It appears to us that the model, coupled with the definition of invariant colors [2], provides an objective way of defining color based entirely upon measurable aspects of the colored chips without resorting to any assumptions about an ideal observer or variations in illuminants.

Taking the cube root of the reflectance spectra has the effect of transforming nonlinear functions into linear functions in the formulation of mathematical models of reflectance spectra. The rules of convex combinations may provide a foundation for formalizing measurement in reflectance spectra space comparable to that provided by Krantz in the formalization of Grassman's laws for monochromatic lights [39,40].

A major puzzle remains, namely, to explain why the reflectance spectra are so well modeled in three-dimensional space. The only reasonable explanation we have found is by Maloney [14], who suggests that it results from some physical constraint imposed on the dimensionality of reflectance spectra by molecular and quantum considerations. The causes of surface and other sources of color are treated by researchers such as Tilley [41] and Nassau [42], but they do not deal explicitly with why reflectance spectra are low dimensional.

ACKNOWLEDGMENTS

We thank Donald D. Hoffman for helpful advice and for suggesting the use of convex combinations and John I. Yellott for bringing the work of H. R. Davidson to our attention.

REFERENCES

1. G. Wyszecki and W. S. Stiles, *Color Science: Concepts and Methods, Quantitative Data and Formulae*, 2nd ed. (Wiley, 1982).
2. F. W. Billmeyer and M. Saltzman, *Principles of Color Technology*, 2nd ed. (Wiley, 1981), pp. 141–142.
3. Munsell Color Company, Inc., *Munsell Book of Color: Matte Finish Collection* (Munsell, 1976).
4. S. M. Newhall, D. Nickerson, and D. B. Judd, "Final report of the OSA. subcommittee on spacing of the Munsell colors," *J. Opt. Soc. Am.* **33**, 385–418 (1943).
5. H. R. Davidson and H. Hemmendinger, "Colorimetric calibration of colorant systems," *J. Opt. Soc. Am.* **45**, 216–219 (1955).
6. T. Indow, "Global color metrics and color appearance systems," *Color Res. Appl.* **5**, 5–12 (1980).
7. T. Indow, "Predictions based on Munsell notation. I. Perceptual color differences," *Color Res. Appl.* **24**, 10–18 (1999).
8. R. G. D'Andrade and A. K. Romney, "A quantitative model for transforming reflectance spectra into the Munsell color space using cone sensitivity functions and opponent process weights," *Proc. Natl. Acad. Sci. U.S.A.* **100**, 6281–6286 (2003).
9. A. K. Romney and T. Indow, "Munsell reflectance spectra represented in three-dimensional Euclidean space," *Color Res. Appl.* **28**, 182–196 (2003).
10. A. K. Romney and R. G. D'Andrade, "Modeling lateral geniculate nucleus cell response spectra and Munsell

- reflectance spectra with cone sensitivity curves," Proc. Natl. Acad. Sci. U.S.A. **102**, 16512–16517 (2005).
11. A. K. Romney and T. Indow, "A model for the simultaneous analysis of reflectance spectra and basis factors of Munsell color samples under D65 illumination in three-dimensional Euclidean space," Proc. Natl. Acad. Sci. U.S.A. **99**, 11543–11546 (2002).
 12. A. K. Romney and J. T. Fulton, "Transforming reflectance spectra into Munsell color space by using prime colors," Proc. Natl. Acad. Sci. U.S.A. **103**, 15698–15703 (2006).
 13. J. Cohen, "Dependency of the spectral reflectance curves of the Munsell color chips," Psychon. **1**, 369–370 (1964).
 14. L. T. Maloney, "Evaluation of linear models of surface spectral reflectance with small numbers of parameters," J. Opt. Soc. Am. A **3**, 1673–1683 (1986).
 15. L. T. Maloney, "Physics-based approaches to modeling surface color perception," in *Color Vision: from Genes to Perception*, K. R. Gegenfurtner and L. T. Sharpe, eds. (Cambridge U. Press, 1999), pp. 387–416.
 16. T. Jaaskelainen, J. Parkkinen, and S. Toyooka, "Vector-subspace model for color representation," J. Opt. Soc. Am. A **7**, 725–730 (1990).
 17. J. L. Dannemiller, "Spectral reflectance of natural objects: how many basis functions are necessary?" J. Opt. Soc. Am. A **9**, 507–515 (1992).
 18. E. L. Krinov, "Spectral reflectance properties of natural formations," translated by G. Beldov (National Research Council of Canada, Technical Translation: TT-439, 1953).
 19. R. Lenz, M. Osterberg, H. Jaaskelainen, and J. Parkkinen, "Unsupervised filtering of color spectra," J. Opt. Soc. Am. A **13**, 1315–1324 (1996).
 20. C. Chiao, T. W. Cronin, and D. Osorio, "Color signals in natural scenes: characteristics of reflectance spectra and effects of natural illuminants," J. Opt. Soc. Am. A **17**, 218–224 (2000).
 21. J. J. Koenderink and A. J. van Doorn, "The structure of colorimetry," in *Algebraic Frames for Perception-Action Cycle*, G. Sommer and Y. Y. Zeevi, eds. (Springer, 2000), pp. 69–77.
 22. R. Lenz and P. Meer, "Non-Euclidean structure of the spectral color space," Proc. SPIE **3826**, 101–112 (1999).
 23. S. Usui, S. Nakauchi, and M. Nakano, "Reconstruction of Munsell color space by a five-layer neural network," J. Opt. Soc. Am. A **9**, 516–520 (1992).
 24. S. A. Burns, J. B. Cohen, and E. N. Kuznetsov, "The Munsell color system in fundamental color space," Color Res. Appl. **28**, 182–196 (2003).
 25. H. Laamanen, T. Jaaskelainen, and J. Parkkinen, "Conversion between the reflectance spectra and the Munsell notation," Color Res. Appl. **31**, 57–66 (2006).
 26. O. Kohonen, J. Parkkinen, and T. Jääskelään, "Databases for spectral color science," Color Res. Appl. **31**, 381–390 (2006).
 27. M. J. Vrhel, R. Gershon, and L. S. Iwan, "Measurement and analysis of object reflectance spectra," Color Res. Appl. **19**, 4–9 (1994).
 28. F. Iova, A. Trutia, and V. Vasile, "Spectral analysis of the color of some pigments," Rom. Rep. Phys. **57**, 905–911 (2005).
 29. M. Elias, C. Chartier, G. Prévot, H. Garay, and C. Vignaud, "The colour of ochres explained by their composition," Mater. Sci. Eng., B **127**, 70–80 (2006).
 30. W. Li-Qin, D. Gao-Chao, W. Xiao-Qi, X. Zhou-Kuan, and L. Guo-Zheng, "Analysis and protection of one thousand hand Buddha in Dazu stone sculptures," Chin. J. Chem. **22**, 172–176 (2004).
 31. A. Ben-Israel and T. N. E. Greville, *Generalized Inverses: Theory and Applications* (Wiley, 1974).
 32. S. Wolfram, *The Mathematica Book*, 4th ed. (Cambridge U. Press, 1999).
 33. T. H. Wonnacott and R. J. Wonnacott, *Regression: A Second Course in Statistics* (Wiley, 1981).
 34. A. Alsam and J. Y. Hardeberg, "Convex reduction of calibration charts," Proc. SPIE **5667**, 38–46 (2005).
 35. A. Alsam and G. Finlayson, "Metamer sets without spectral calibration," J. Opt. Soc. Am. A **24**, 2505–2512 (2007).
 36. S. P. Gudder, "Convexity and mixtures," SIAM Rev. **19**, 221–240 (1977).
 37. J. C. Maxwell, "Theory of the perception of colors," Trans. R. Scottish Soc. Arts. **4**, 394–400 (1856); reprinted as *Sources of Color Science*, D. L. MacAdam, ed. (MIT, 1970).
 38. H. R. Davidson, "Formulations for the OSO Uniform Color Scales committee samples," Color Res. Appl. **6**, 38–52 (1981).
 39. D. H. Krantz, "Fundamental measurement of force and Newton's first and second laws of motion," Philos. Sci. **40**, 481–495 (1973).
 40. D. H. Krantz, "Color measurement and color theory. 1. Representation theorem for Grassmann structures," J. Math. Psychol. **12**, 283–303 (1975).
 41. R. J. D. Tilley, *Colour and Optical Properties of Materials* (Wiley, 2000).
 42. K. Nassau, *The Physics and Chemistry of Color*, 2nd ed. (Wiley, 2001).